Numerical Performances of the SIR Dynamical Prototype with the Hospital Bed Impacts Using Artificial Neural Network

Sadaf Irshad[1], Sohaib Latif[2*], Daniyal Affandi[3], Saher Pervaiz[4]

[1]*School of Mathematics and Big Data, Anhui University of Science and Technology, China*
[2]*Department of Computer Science and Software Engineering, Grand Asian University, Pakistan.*
[3,4]*Department of Computer Science, University of Chnab, Pakistan*
**Email: sohaiblatif095@gmail.com*

Graphical Abstract:

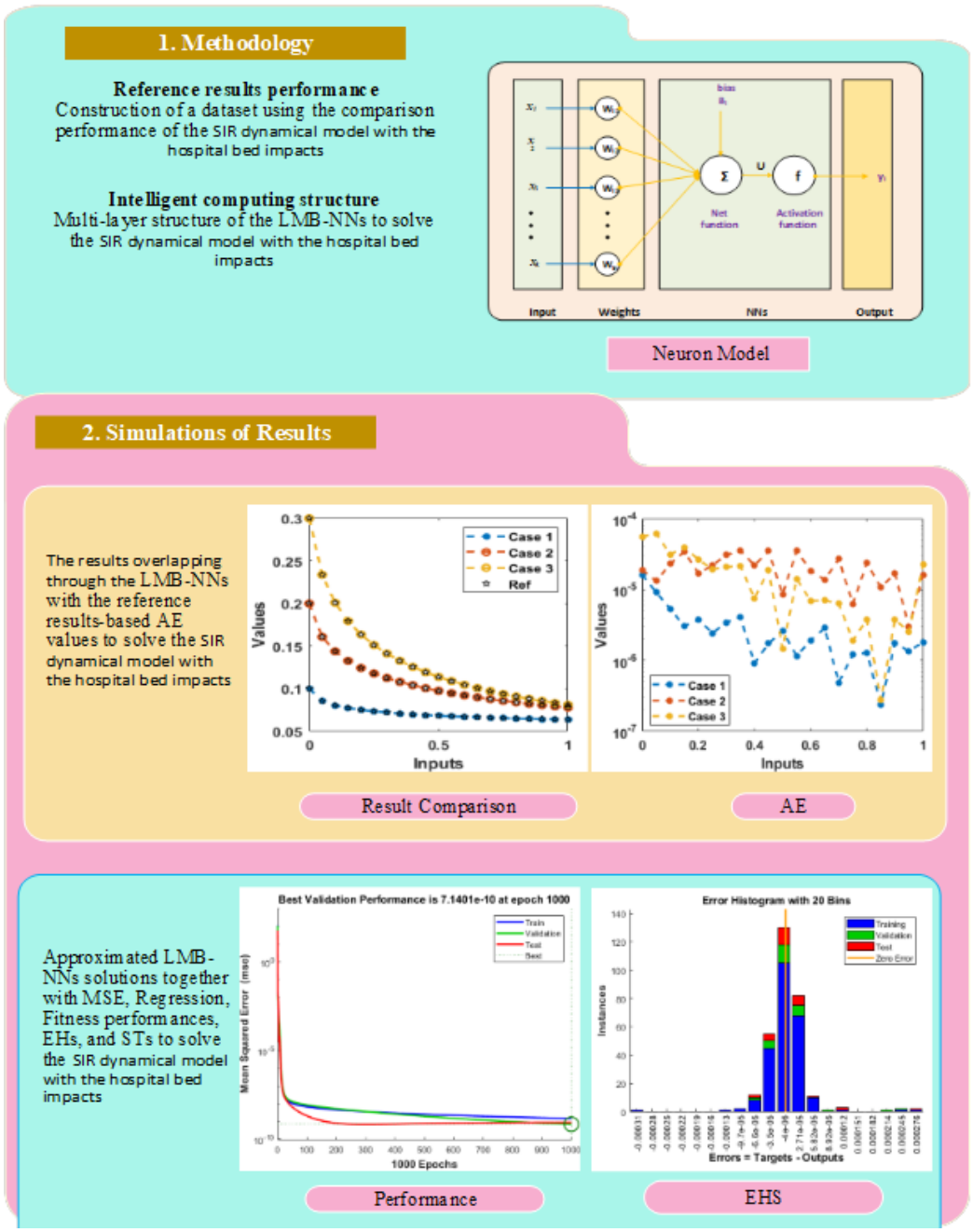

Abstract: This study is conducted to check the behavior of SEIR model based on the Levenberg-Marquardt backpropagation (LMQB) along with the neural networks (NN) i.e., LMQB neural networks describes the mathematical evaluation of SEIR model with available number of bed in hospitals. The epidemic SEIR model works on four dimensions, where S is the number of susceptible people who are admitted in hospital. E is represented the number of exposed persons, I shows the infected persons and R indicates the recovered persons respectively. The numerical findings are evaluated through LMQB neural networks. These findings are measured for the four dimensions of SEIR model by taking the data samples, training of dataset, authentication, and testing the results. The results show the metrics are selected as 70% for dataset training, 18% for confirmation and 12% for testing. The theoretical analysis is presented to show the numerical modeling. The SEIR model outcome is described using LMQB neural networks to overcome the mean square error (MSE). The numerical results are described using the LMQB neural networks through the MSE, error histograms (EHs), state transitions (STs), regression and correlation for attaining the correctness, consistency, capability, and productivity.

Keywords: SEIR model; Nonlinear system; LMQB; E-health system; Machine Learning Techniques.

1. Introduction

Stochastic processes are mathematical objects used to model systems or phenomena that evolve over time in a way that is inherently random. They are fundamental in various fields such as finance, physics, biology, and engineering due to their ability to represent uncertainty and random variability. In finance, stochastic processes are employed to model stock prices, interest rates, and market risks. The famous Black-Scholes model for option pricing, for instance, relies on stochastic calculus to predict the future prices of financial derivatives. In physics, stochastic processes describe the random motion of particles, known as Brownian motion, which is pivotal in the study of diffusion processes and statistical mechanics. They help explain how particles spread through a medium, which has implications in various branches of physics and chemistry. In biology, stochastic models are used to represent the randomness in population dynamics, genetic drift, and the spread of diseases. These models help in understanding how biological systems change over time in the presence of random fluctuations. In engineering, stochastic processes are essential in the analysis and design of communication systems, where they model the noise and interference affecting signal transmission. They are also crucial in the reliability analysis of complex systems, predicting the likelihood of system failures over time. Stochastic processes provide a versatile framework for modeling and analyzing systems influenced by randomness, enabling researchers and practitioners to make informed predictions and decisions in the face of uncertainty.
Stochastic solvers have found applications in many recent and advanced fields, particularly in machine learning and data science. One notable application is in reinforcement learning, a type of machine learning where agents learn to make decisions by interacting with an environment. In this context,

stochastic processes are used to model the environment's uncertainty and variability. Algorithms like Q-learning and Monte Carlo methods rely on stochastic solvers to estimate the value of different actions under uncertainty, enabling the development of sophisticated AI systems capable of playing complex games, optimizing industrial processes, or even managing autonomous vehicles. These solvers help in dealing with the randomness and noise in the data, improving the robustness and performance of the learning algorithms. The growing field of stochastic optimization in deep learning also leverages these solvers to efficiently train large neural networks by navigating the high-dimensional and non-convex loss landscapes.

Viruses are spreading rapidly across the globe in which coronavirus is at the top. The proper treatment is needed to overcome the spread of these viruses which is suitable and effective way of controlling viruses. The outbreak is controlled by treatment function shows the probability of affected population [1]. The probability also shows that how many affected population has received the treatment at a given time. In many conventional models, treatment rates are considered to be proportional to the number of affected people. In everywhere, the medical resources are very limited for the cure of these viruses [2]. That's why we have lost many lives due to shortage of resources and also non availability of planning against any uncertain outbreak.

This study proposes a SEIR outbreak model which assumes the data of susceptible, exposed, infectious and recovered patients. The data shows that the dynamics are limited to some area and also changes over time [3]. The dynamics, despite their simplicity, have a wide range of dynamical behavior, from steady equilibrium themes to episodic. The bifurcation is becoming popular and vibrant in research and practical applications [4]. In our daily routine life, we are practicing many applications of discrete systems that are the biggest achievement in the field of quantum mechanics, engineering, and mathematics [5]. Using the Euler difference approach, Hu et al. [6] introduced a new epidemic model and studied the Neimark-Sacker bifurcation is rely on center manifold theorem and bifurcation theory. Pitchfork bifurcation, Flip bifurcation, and Neimark-Sacker bifurcation of a two-dimensional discrete Lorenz system were investigated by Elabbasy et al. [7]. He analyzes the existence and direction of the system's Neimark-Sacker bifurcation, which is a third-order rational difference equation with positive parameters.

There are many SEIR outbreak models based on nonlinear mathematical system that have been introduced, few of them are Efimov, D. and Ushirobira, R. [8], De la Sen, M., Alonso-Quesada, S. and Ibeas, A. [9], Marinca, B., Marinca, V. and Bogdan, C., [10], Meng, L. and Zhu, W., [11], Kumar, Ajay, et al. [12], Naim, Mouhcine, et al. [13], Abbasi, Zohreh, et al. [14], Sen, Manuel De la, et al. [15], Kumar, Sunil, et al. [16], Jin, Manli, and Yuguo Lin. [17], Bajiya, Vijay Pal, et al.[18], Senel, Li, Yan, Xinyu Zhang, and Han Cao. [19] and De la Sen, M., and A. Ibeas. [20].

Outbreak is usually spread from person to person, person to animals or animals to animals. The dynamics of infectious disease have seen significant progress since the mid-twentieth century, and outbreak dynamical models have been extensively studied [21]. Mostly discrete system bifurcation research is focused on two-dimensional systems, with only a few studies concentrating on three-dimensional discrete systems. However, in comparison the three dimensional model give better performance as compared to the two-dimensional model of infectious diseases [22]. Table 1 described the abbreviations of SEIR dynamic prototype.

Table 1: Suitable description for the SIR dynamical prototype

Parameter	Descriptions
$S(\omega)$	Susceptible
$E(\omega)$	Number of exposed persons
$I(\omega)$	Infected persons admitted in hospital
$R(\omega)$	Number of patients recovered after treatment
β	Average number of adequate contacts per unit time
μ	Recovery rate of infected persons
A	Recruitment rate of susceptible population
d	Natural death rate of the population
ν	Disease-induced death rate
ω	Time

This work is to explain the highly nonlinear SIR dynamical prototype using the stochastic computing based on LMB-NNs. The numerical performances are presented using the selection of the data as 74% for dataset training, 15% for confirmation and 11% for testing. The stochastic computing explainers have been explored to explain the various grim and challengeable dynamics in the field of singular prototypes, fractional order systems, pantograph prototypes, biological systems, prediction differential systems, and functional differential systems, food chain systems economic and environmental prototypes [26]. These motivational investigations impressed the authors to present the numerical performances of the SIR dynamical prototype. Few novelty factors of this study are described below as:

- A numerical procedural LMB-NNs form is presented to explain the SIR dynamical prototype.
- The effective results have been obtained using the LMB-NNs for solving the nonlinear SIR dynamical prototype.
- The correctness of the computational numerical procedural LMB-NNs form is observed by using the comparison procedures of the proposed and reference solutions.
- The effective absolute error (AE) performances have also been calculated in good ranges that depicts the exactness of the computational numerical LMB-NNs
- The reliability and performance of the computational numerical LMB-NNs explain for the SIR dynamical prototype is observed by using M.S.E, STs, EHs, and regression and correlation gages.

The rest of the work is organized as follows: Section 2 discusses the methodology of the LMB-NNs for SIR dynamical prototype. The numerical simulations are discussed in the 3rd Section. Conclusion and future work of this study is presented in 4th Section. The paper is organized as follows. In section 2, we discuss the stability of fixed points and the Hopf bifurcation. The stability of fixed points and the existence, direction and stability of the Hopf bifurcation of the discretized system are investigated in section 3. In section 4, we present the numerical simulations illustrate our results with the theoretical analysis. We have given some comparisons of bifurcation between the continuous-time epidemic system and its discrete-time system in section 5. In section 6, conclusion of the paper is given.

2. Methodology

The proposed LMB-NNs are described in two phases to explain all three sessions of the SIR dynamical prototype in this section. Fig 1 shows an acceptable optimization approach for multi-layer actions using LMB-NNs. The proposed prototype using a single neuron. The LMB-NNs technique is carried out using 'nftool' (a Matlab built-in command) and is based on the proportions of these data i.e., 74% for dataset training, 15% for confirmation and 11% for testing.

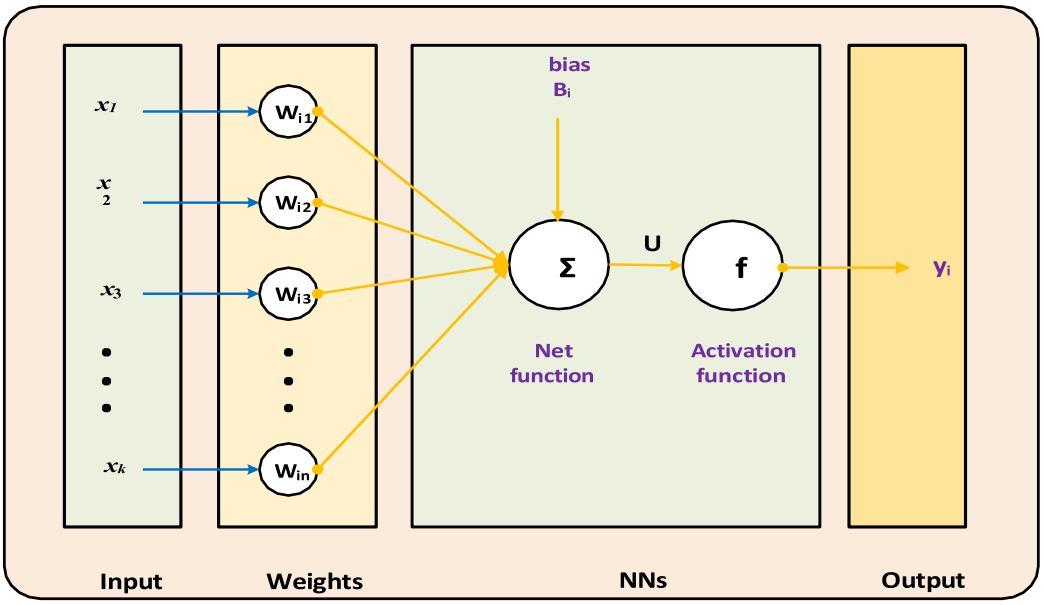

Fig 1: Structural view of single neuron

3. Results

The mathematical findings are represented for the SIR dynamical prototype relies on its three types. The mathematical form using the LMB-NNs is given as:

Case-1: Consider the SIR dynamical prototype with the appropriate values $A = 20$, $\mu\left(b, I(\omega)\right) = \mu_0 = 10$, $d = 0.1$, $\upsilon = 1$ and $\beta = 11.5$ along with the ICs 0.1, 0.1 and 0.1 is given as:

(1)

Case-2: Consider the SIR dynamical prototype with the appropriate values $A = 20$, $\mu\left(b, I(\omega)\right) = \mu_0 = 10$, $d = 0.1$, $\upsilon = 1$ and $\beta = 11.5$ along with the ICs 0.2, 0.2 and 0.2 is given as:

$$\begin{cases} \dfrac{dS(\omega)}{d\omega} = 20 - 0.1S(\omega) - \dfrac{11.5S(\omega)I(\omega)}{S(\omega)+I(\omega)+R(\omega)}, & S(0) = 0.2, \\ \dfrac{dI(\omega)}{d\omega} = -1.1I(\omega) - 10I(\omega) + \dfrac{11.5S(\omega)I(\omega)}{S(\omega)+I(\omega)+R(\omega)} & I(0) = 0.2, \\ \dfrac{dR(\omega)}{d\omega} = 10I(\omega) - 0.1R(\omega), & R(0) = 0.2. \end{cases} \quad (2)$$

Case-3: Consider the SIR dynamical prototype with the appropriate values $A = 20$, $\mu\left(b, I(\omega)\right) = \mu_0 = 10$, $d = 0.1$, $\upsilon = 1$ and $\beta = 11.5$ along with the ICs 0.3, 0.3 and 0.3 is given as:

$$\begin{cases} \dfrac{dS(\omega)}{d\omega} = 20 - 0.1S(\omega) - \dfrac{11.5S(\omega)I(\omega)}{S(\omega)+I(\omega)+R(\omega)}, & S(0) = 0.3, \\ \dfrac{dI(\omega)}{d\omega} = -1.1I(\omega) - 10I(\omega) + \dfrac{11.5S(\omega)I(\omega)}{S(\omega)+I(\omega)+R(\omega)} & I(0) = 0.3, \\ \dfrac{dR(\omega)}{d\omega} = 10I(\omega) - 0.1R(\omega), & R(0) = 0.3. \end{cases} \quad (3)$$

The mathematical calculations are performed to explain the SIR dynamical prototype based on the LMB-NNs with input [0, 1] with the step size of 0.01. The proposed LMB-NNs are taken huge part of the data using the statistics, i.e., 74% for dataset training, 15% for confirmation and 11% for testing. In this study, amount of neurons are taken 8 for the nonlinear SIR dynamical system.

The illustrations of the LMB-NNs to explain each session of the nonlinear SIR dynamical system are presented in Figs 2 and 3. The accomplished performance and transition states are explained in all session of the nonlinear SIR dynamical system is provided in Figs 2. The derived measures for testing, training, best curves, and confirmations using the MSE are shown in Fig 2(a-c) to explain the nonlinear SIR dynamical system. The best performances to explain each group of the nonlinear SIR dynamical prototype at epoch 1000 calculated almost 4.71 ×10 10, 1.334 ×10 11 and 5.71 ×10 12. Fig 2(d-f) shows the gradient values using the LMB-NNs to describe the nonlinear SIR dynamical prototype is around 1.64 × 10-06, 7.37 × 10-07 and 2.68 × 10-06. The values in Figs show the correctness and precision to describe the individual session of the nonlinear SIR dynamical system. In Figs 3(a-c), the fitting curve plots to explain individual session of the nonlinear SIR dynamical system is provided. The plots based on the EHs are derived in Fig 3(d-f); it is observed that the EHs are found around 2.7 × 10-05, 5.5 × 10-06 and 3.6 × 10-07. In individual session of the SIR dynamical system the correlation

values are observed 1 in ideal case. The dataset training, conformance and testing represent the correctness and precision of the LMB-NNs to explain individual session of the nonlinear SIR dynamical prototype as shown in Table 1.

Table 1: LMB-NNs performances to explain nonlinear SIR dynamical system

Case	MSE			Gradient	Performance	Epoch	Mu	Time
	Training	Testing	Confirmation					
1	1.50×10^{-09}	7.14×10^{-10}	8.98×10^{-10}	1.34×10^{-06}	1.51×10^{-09}	1000	1×10^{-08}	06
2	1.77×10^{-09}	4.44×10^{-09}	4.53×10^{-10}	1.55×10^{-06}	1.77×10^{-09}	1000	1×10^{-07}	06
3	4.71×10^{-10}	5.65×10^{-09}	5.34×10^{-10}	9.33×10^{-07}	4.71×10^{-10}	1000	1×10^{-08}	06

(a) Case 1: MSE

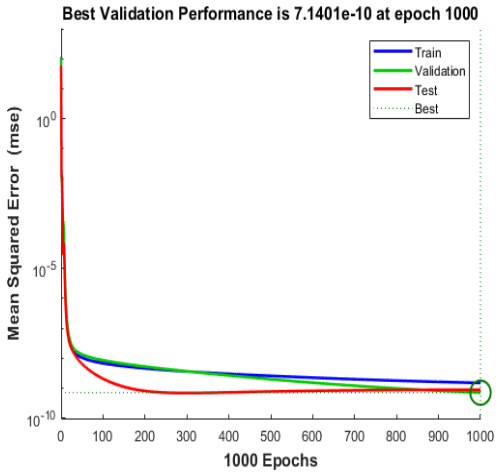

(d) Case I: ST values

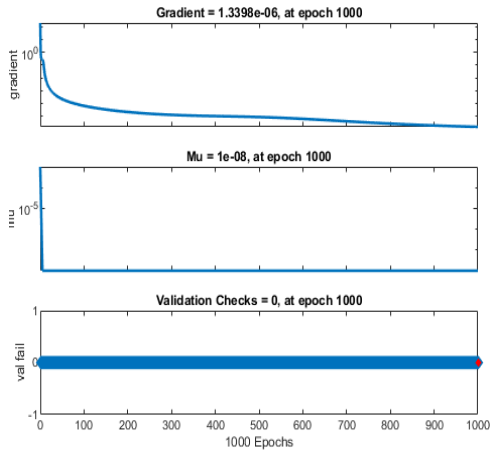

(b) Case 2: MSE

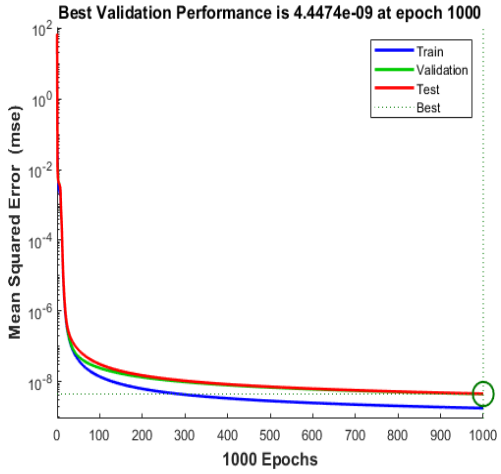

(e) Case 2: State transition values

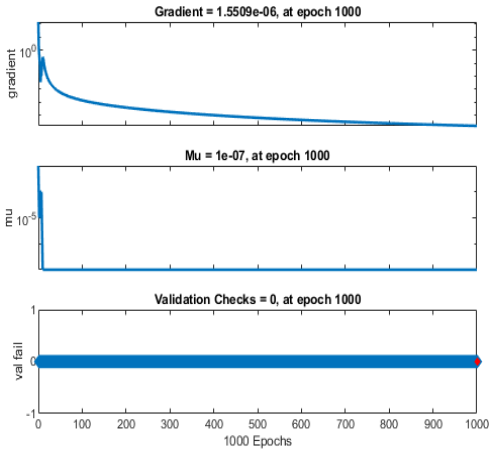

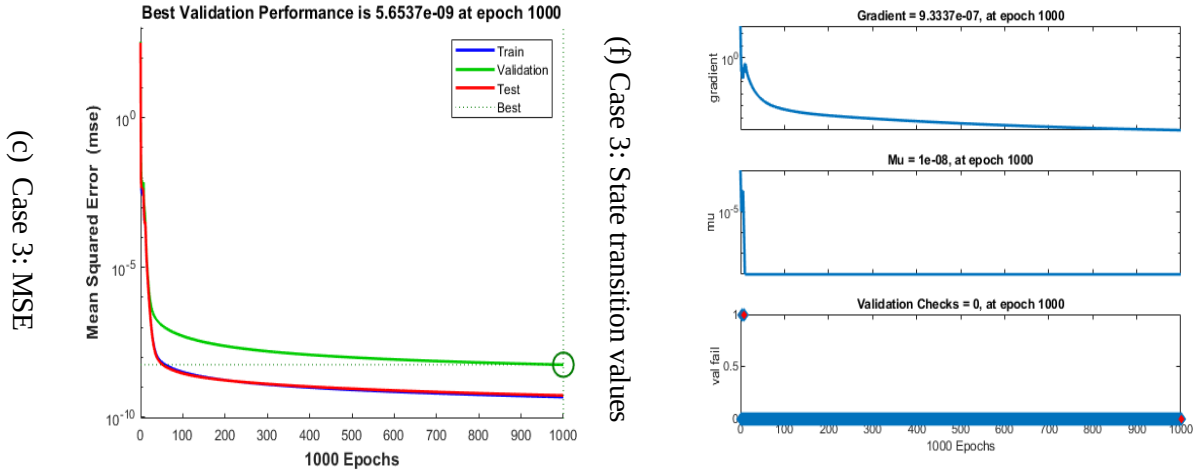

(c) Case 3: MSE (f) Case 3: State transition values

Fig 2: MSE Performances (a-c) and State transition values (d-f) to explain nonlinear SIR dynamical prototype

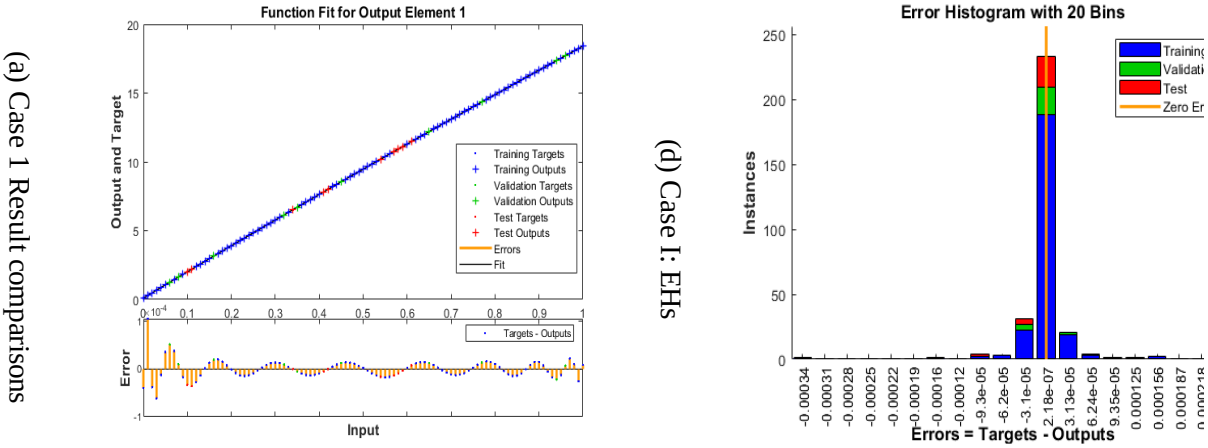

(a) Case 1 Result comparisons (d) Case I: EHs

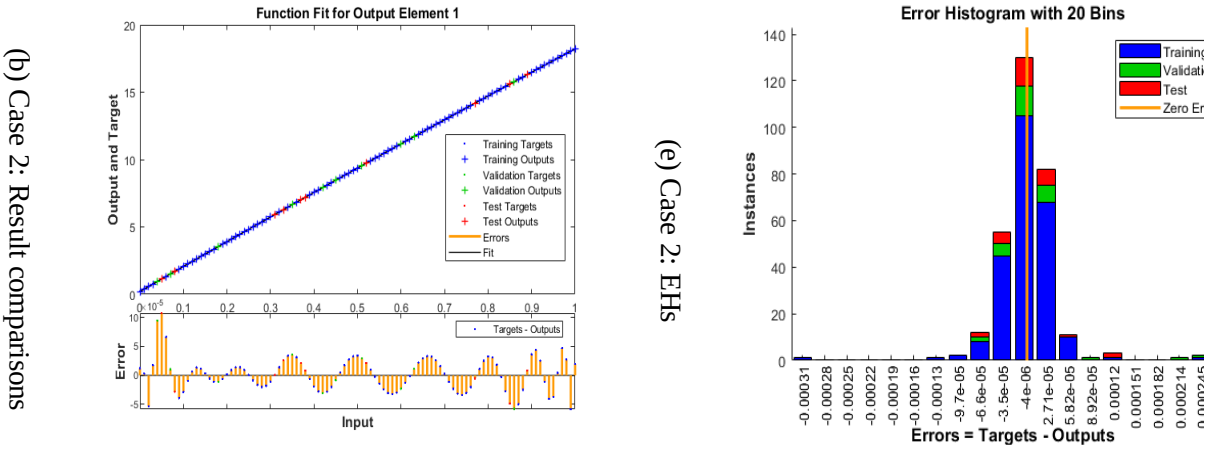

(b) Case 2: Result comparisons (e) Case 2: EHs

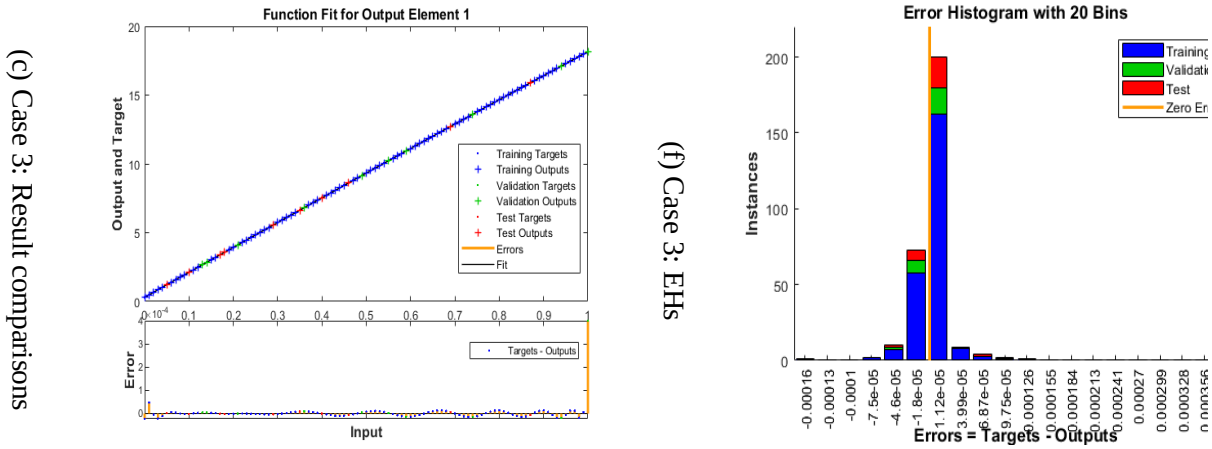

Fig 3: Comparison of results and EHs for the nonlinear SIR dynamical system

The comparison plots are provided in Figs 4 and 5 based on the nonlinear dynamical SIR system. The results of the categories $S(\omega)$, $I(\omega)$ and $R(\omega)$ using the LMB-NNs are drawn in subfigures 4(a-c). The exact overlapping of the solutions (reference and obtained) expresses the precision and exactness of the LMB-NNs for solving the SIR dynamical system. The AE performances are drawn in Fig 5 to expressed each category of the system. These measures $S(\omega)$, $I(\omega)$ and $R(\omega)$ using the LMB-NNs are plotted in subfigures 5. Fig 5(a) illustrates the AE for $S(\omega)$ calculated as 10^{-04} to 10^{-06}, 10^{-04} to 10^{-07} and 10^{-05} to 10^{-08} for cases 1, 2 and 3. Fig 5(b) illustrates the AE for $I(\omega)$ calculated as 10^{-03} to 10^{-06}, 10^{-04} to 10^{-06} and 10^{-04} to 10^{-07} for cases 1, 2 and 3. Fig 5(c) illustrates the AE for $R(\omega)$ calculated as 10^{-05} to 10^{-07}, 10^{-04} to 10^{-06} and 10^{-05} to 10^{-06} for cases 1, 2 and 3. These close identical values indicates the correctness of the LMB-NNs for each class of the nonlinear SIR dynamical prototype.

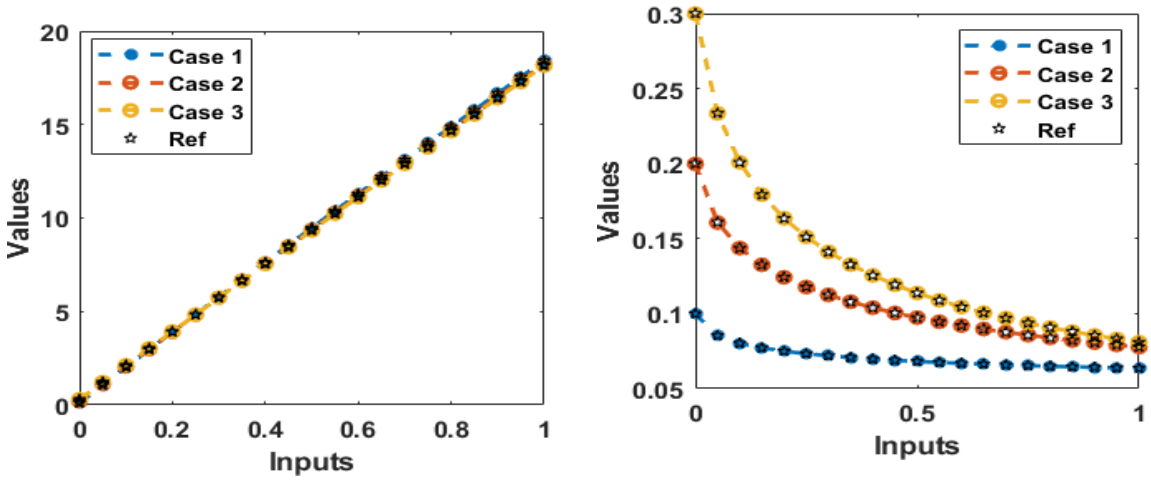

(a) Results of Sh class

(b) Results of Ih class

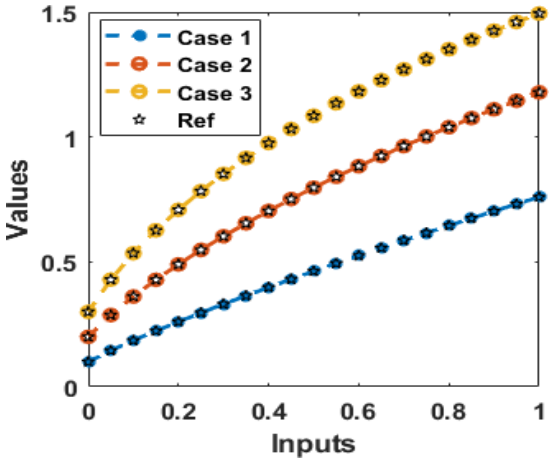

(c) Results of P class

Fig 4: Comparison plots through the LMB-NNs to explain nonlinear SIR dynamical prototype

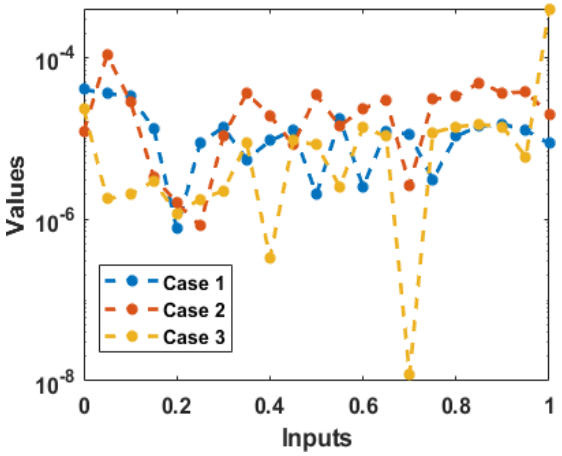

(a) AE for Sh class

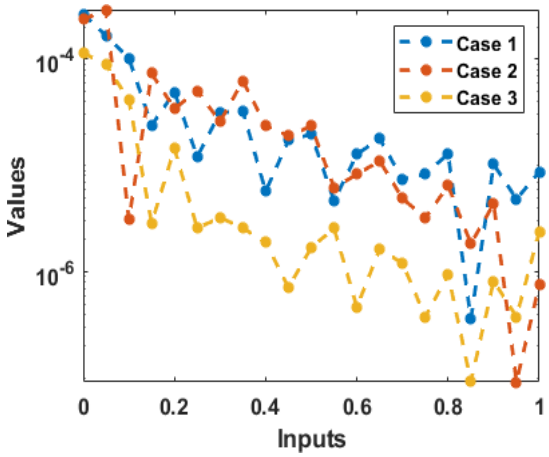

(b) AE for Ih class

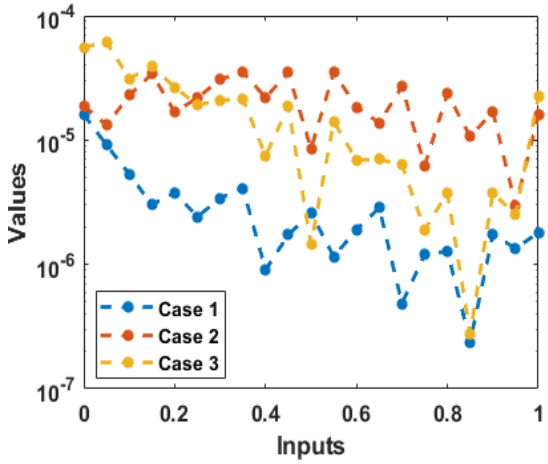

(c) AE for P class

Fig 5: AE values through the LMB-NNs to explain nonlinear SIR dynamical prototype

4. Conclusions

The aim of this study is to develop a stochastic computing analyzer relies on the Levenberg-Marquardt backpropagation neural networks. In this study, an SIR dynamical prototype is presented. The SIR dynamical prototype relies on three categories: susceptible patients of hospital, infected persons and recovered population. The three diverse categories of the nonlinear SIR dynamical prototype are mathematically implemented by the LMB-NNS using the dataset training, confirmation, verification, and testing. The three SIR dynamical prototype categories have been taken based on the prediction rate. The statics are selected as 74% for dataset training, 15% for confirmation and 11% for testing. The

results are compared with reference solutions for authentication and verification. In this way, the absolute error is obtained very accurate that is around 10^{-06} to 10^{-10} for individual session of the nonlinear SIR dynamical system. The LMB-NNs are used to describe the performance of the produced outcomes in order to reduce the mean square error. The mathematical findings employing proportional measures through the MSE, error histograms (EHs), and regression/correlation are also performed for the correctness, dependability, competency, and efficiency of the LMB-NNs. This study proposes the LMB-NNs is stable and calculate the nonlinear system of equations more accurately.
In the future, we embedded the proposed LMB-NNs to evaluate the mathematical solutions of the fluid dynamics systems, environmental and economic prototypes and nonlinear singular systems.

References

[1] Li, T., Zhang, F., Liu, H. and Chen, Y., 2017. Threshold dynamics of an SIRS prototype with nonlinear incidence rate and transfer from infectious to susceptible. Applied Mathematics Letters, 70, pp.52-57.

[2] Sánchez, Y.G., Sabir, Z. and Guirao, J.L., 2020. Design of a nonlinear SITR fractal prototype based on the dynamics of a novel coronavirus (COVID-19). Fractals, 28(08), p.2040026.

[3] Li, J., Yang, Y., Xiao, Y. and Liu, S., 2016. A class of Lyapunov functions and the global stability of some epidemic prototypes with nonlinear incidence. Journal of Applied Analysis & Computation, 6(1), pp.38-46.

[4] Cao, H., Wu, H. and Wang, X., 2020. Bifurcation analysis of a discrete SIR epidemic prototype with constant recovery. Advances in Difference Equations, 2020(1), pp.1-20.

[5] Cui, Q., Qiu, Z., Liu, W. and Hu, Z., 2017. Complex dynamics of an SIR epidemic prototype with nonlinear saturate incidence and recovery rate. Entropy, 19(7), p.305.

[6] Hethcote, H.W., 2000. The mathematics of infectious diseases. SIAM review, 42(4), pp.599-653.

[7] Liu, L., 2015. A delayed SIR prototype with general nonlinear incidence rate. Advances in Difference Equations, 2015(1), pp.1-11.

[8] Fan, X., Wang, L. and Teng, Z., 2016. Global dynamics for a class of discrete SEIRS epidemic prototypes with general nonlinear incidence. Advances in difference equations, 2016(1), pp.1-20.

[9] Weiss, H.H., 2013. The SIR prototype and the foundations of public health. Materials mathematics, pp.0001-17.

[10] Ji, C. and Jiang, D., 2014. Threshold behaviour of a stochastic SIR prototype. Applied Mathematical Prototypeling, 38(21-22), pp.5067-5079.

[11] Cooper, I., Mondal, A. and Antonopoulos, C.G., 2020. A SIR prototype assumption for the spread of COVID-19 in different communities. Chaos, Solitons & Fractals, 139, p.110057.

[12] Acemoglu, D., Chernozhukov, V., Werning, I. and Whinston, M.D., 2020. Optimal targeted lockdowns in a multi-group SIR prototype (No. w27102). National Bureau of Economic Research.

[13] Zhu, K. and Ying, L., 2014. Information source detection in the SIR prototype: A sample-path-based approach. IEEE/ACM Transactions on Networking, 24(1), pp.408-421.

[14] Elsonbaty, A., et al., 2021. Dynamical analysis of a novel discrete fractional SITRS prototype for COVID-19. Fractals, p.2140035.

[15] Smith, D. and Moore, L., 2004. The SIR prototype for spread of disease-the differential equation prototype. Convergence.

[16] Kudryashov, N.A., Chmykhov, M.A. and Vigdorowitsch, M., 2021. Analytical features of the SIR prototype and their applications to COVID-19. Applied Mathematical Prototypeling, 90, pp.466-473.

[17] Chen, X., Li, J., Xiao, C. and Yang, P., 2021. Numerical solution and parameter estimation for uncertain SIR prototype with application to COVID-19. Fuzzy Optimization and Decision Making, 20(2), pp.189-208.

[18] Gatto, N.M. and Schellhorn, H., 2021. Optimal control of the SIR prototype in the presence of transmission and treatment uncertainty. Mathematical Biosciences, 333, p.108539.

[19] Alshammari, F.S. and Khan, M.A., 2021. Dynamic behaviors of a modified SIR prototype with nonlinear incidence and recovery rates. Alexandria Engineering Journal, 60(3), pp.2997-3005.

[20] Senel, K., Ozdinc, M. and Ozturkcan, S., 2021. Single parameter estimation approach for robust estimation of SIR prototype with limited and noisy data: the case for COVID-19. Disaster Medicine and Public Health Preparedness, 15(3), pp.e8-e22.

[21] Sabir, Z., et al., 2020. Numerical investigations to design a novel prototype based on the fifth order system of Emden–Fowler equations. Theoretical and Applied Mechanics Letters, 10(5), pp.333-342.

[22] Elsonbaty, A., et al., 2021. Dynamical analysis of a novel discrete fractional SITRS prototype for COVID-19. Fractals, p.2140035.

[23] Guerrero Sánchez, Y. et al., 2020. Analytical and approximate solutions of a novel nervous stomach mathematical prototype. Discrete Dynamics in Nature and Society, 2020.

[24] Sánchez, Y.G., et al., 2020. Design of a nonlinear SITR fractal prototype based on the dynamics of a novel coronavirus (COVID-19). Fractals, 28(08), p.2040026.

[25] Suryaningrat, W. et al., 2020, September. The optimal control of rice tungro disease with insecticide and

biological agent. In AIP Conference Proceedings (Vol. 2264, No. 1, p. 040002). AIP Publishing LLC.
[26] Latif, S., Sabir, Z., Raja, M.A.Z., Altamirano, G.C., Núñez, R.A.S., Gago, D.O., Sadat, R. and Ali, M.R., 2023. IoT technology enabled stochastic computing paradigm for numerical simulation of heterogeneous mosquito model. Multimedia Tools and Applications, 82(12), pp.18851-18866.